Mechanism of Focal Adhesion Kinase Mechanosensing

Jing Zhou[1]◉, Camilo Aponte-Santamaría[1]◉, Sebastian Sturm[2], Jakob Tómas Bullerjahn[2], Agnieszka Bronowska[1], Frauke Gräter[1,3]*

1 Heidelberg Institute for Theoretical Studies, Heidelberg, Germany, **2** Leipzig University, Institute for Theoretical Physics, Leipzig, Germany, **3** Interdisciplinary Center for Scientific Computing (IWR), Heidelberg University, Heidelberg, Germany

◉ These authors contributed equally to this work.
* frauke.graeter@h-its.org

Abstract

Mechanosensing at focal adhesions regulates vital cellular processes. Here, we present results from molecular dynamics (MD) and mechano-biochemical network simulations that suggest a direct role of Focal Adhesion Kinase (FAK) as a mechano-sensor. Tensile forces, propagating from the membrane through the PIP_2 binding site of the FERM domain and from the cytoskeleton-anchored FAT domain, activate FAK by unlocking its central phosphorylation site (Tyr576/577) from the autoinhibitory FERM domain. Varying loading rates, pulling directions, and membrane PIP_2 concentrations corroborate the specific opening of the FERM-kinase domain interface, due to its remarkably lower mechanical stability compared to the individual alpha-helical domains and the PIP_2-FERM link. Analyzing downstream signaling networks provides further evidence for an intrinsic mechano-signaling role of FAK in broadcasting force signals through Ras to the nucleus. This distinguishes FAK from hitherto identified focal adhesion mechano-responsive molecules, allowing a new interpretation of cell stretching experiments.

Author Summary

Focal adhesions integrate external mechanical signals into biochemical circuits allowing cellular mechanosensing. Although the zoo of mechanosensing proteins at focal adhesions is steadily growing, force-induced enzymatic mechanisms, as those uncovered for autoinhibited kinases in muscle, remain to be identified for focal adhesion downstream signaling. Here, we provide evidence that focal adhesion kinase (FAK) can act as a direct mechano-enzyme at focal adhesions, using molecular dynamics simulations and kinetic modelling. We show that anchorage of FAK to the membrane via PIP-2 is critical for this mechanical activation. Our results suggest similar mechanisms to be at play for other membrane-bound autoinhibited kinases.

Introduction

Focal adhesions (FAs) act as key cellular locations for mechanosensing by integrating mechanical and biochemical signals between the outside and inside of the cell, thereby regulating processes such as cell proliferation, motility, differentiation, and apoptosis [1–3]. They contain numerous adapter or anchor proteins, which establish the mechanical link of the cytoskeleton with the extracellular matrix [4]. Some of these proteins have been identified as mechano-responsive elements [5–7].

Focal Adhesion Kinase (FAK) centrally regulates FAs by establishing adhesive interactions at the cell periphery [8]. Acting as a signaling hub between integrin and multiple proteins participating in downstream signaling pathways, it carries out diverse functions in embryonic development, cell migration, and survival, and its malfunction is associated with cancer progression and cardiovascular diseases [9, 10]. FAK comprises a central tyrosine kinase domain flanked by two large non-catalytic domains: FERM and FAT (Fig 1A). The N-terminal three-lobed 4.1 ezrin radixin moesin (FERM) homology domain is connected to the kinase N-lobe
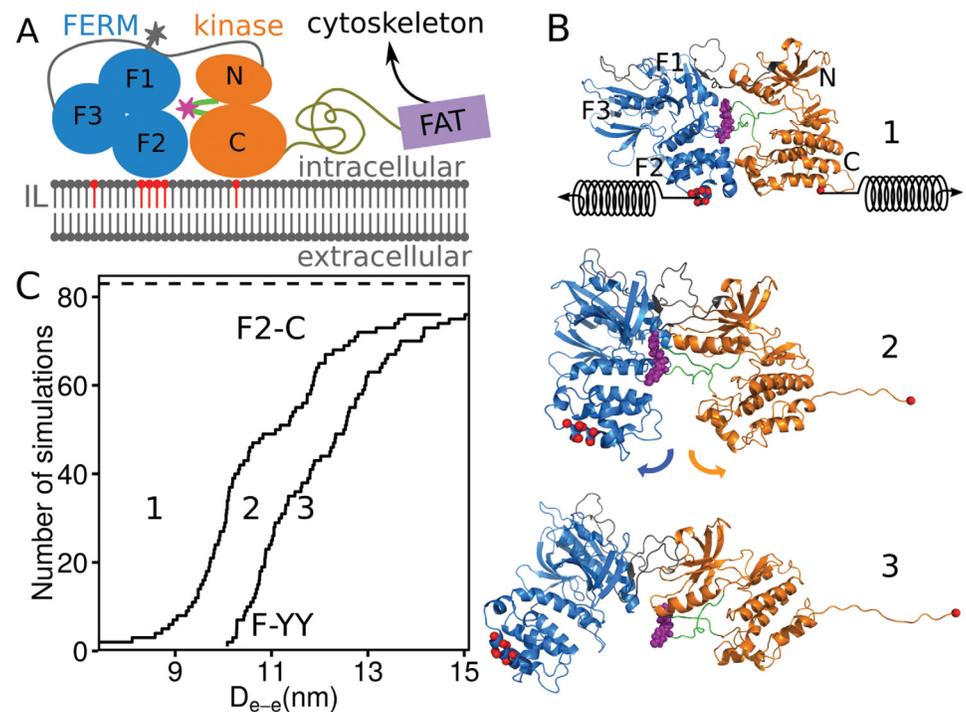
Fig 1. Mechanical activation of FK-FAK. A) Domain organization of FAK and its relative position at the cell periphery in the cytosol. The kinase domain (orange) contains the lobes N and C and the FERM domain (blue) consists of lobes F1–3, with F2 binding to PIP$_2$ lipids (red) concentrated at the inner leaflet (IL) of the membrane (grey). The major phosphorylation site Tyr576/577 (magenta star), located at the activation loop (green) in the kinase domain, is autoinhibited by the FERM domain. The autophosphorylation site Tyr397 (grey star) is positioned in the loop connecting the kinase and FERM domains (grey). The FAT domain (violet) is not considered in our study. B) Stretching force applied to the basic patch in FERM and the kinase C-terminal residue (red), in form of virtual springs, induces FERM-kinase dissociation. Representative structures of FAK in its initial autoinhibited conformation (1), after dissociation of the kinase C-lobe from the FERM F2 lobe (2), and after Tyr576/577 release and partial C-terminal unfolding (3) are shown. Color-code and orientation of the protein as in A. C) Cumulative number of dissociation events as a function of the distance between the pulled elements at the moment of dissociation (D_{e-e}). This indicates the extent of unfolding prior dissociation. Two events were monitored: dissociation of the the FERM F2 lobe from the kinase C-lobe, F2-C (transition from (1) to (2) in B), and separation of FERM domain from the Tyr576–577 phosphorylation site, F-YY (transition from (2) to (3) in B). Total number of simulations (83) is indicated with the dashed line.

doi:10.1371/journal.pcbi.1004593.g001

through a 50-residue linker. The C-terminal FAT (focal adhesion targeting) domain follows a 220-residue long proline-rich and disordered linker, through which it is connected to the kinase C-lobe. The activation of FAK first requires autophosphorylation of Tyr397, which offers a Src homology 2 (SH2) binding site. Src binding to FAK increases Src kinase activity, inducing the phosphorylation of Tyr576/577 within the kinase domain activation loop [11]. This is needed for maximal FAK-associated activity and leads to the formation of a Src-FAK complex, which triggers subsequent phosphorylations in the FAT domain and binding of downstream signaling proteins [12]. The FERM domain auto-inhibits the kinase domain by blocking the Tyr576/577 phosphorylation site [13, 14]. Exposure of this site is an essential step to permit its phosphorylation, and thereby render maximum FAK activity.

FAK locates at sites of integrin clustering through protein-protein interactions of its FAT domain, which contains binding sites for integrin- and actin-associated proteins [4, 15]. Integrin signaling and interactions with growth factor receptors were determined as FAK activators [16, 17]. Recent studies provided evidence that phosphoinositide phosphatidylinsositol-4,5-bis-phosphate (PIP_2) is critical for efficient FAK activation and autophosphorylation [18, 19]. PIP_2, a ubiquitous second messenger enriched in the inner leaflet of the plasma membrane and concentrated at FAs, regulates the interaction of cytoskeletal proteins with the membrane [20, 21]. PIP_2 interacts directly with the basic patch (^{216}KAKTLR^{221}) in the FERM domain [18, 19], which induces conformational changes in FAK. The global concentration of PIP_2 in the cell membrane is only approximately 1% [22]. However, PIP_2-protein interactions [22, 23] or divalent ions, such as Ca^{2+}, [24, 25] can lead to local PIP2 accumulation. Localized increments of Ca^{2+} were also suggested to increase the residency of FAK at FAs [26].

Evidence for a decisive role of FAK in mechanotransduction is steadily growing [27]. FAK is recruited to the leading edge and phosphorylated in migrating cells under shear stress [28, 29]. It has also been shown to mediate force-guided cell migration [30, 31] as well as strain-induced proliferation [32]. Recently, the mechano-sensitivity of FAK has been ascribed to the force-sensing fibronectin-integrin link [33]. However, until now, the available data on mechano-sensing through FAK is indirect. It remains unknown if FAK only lies downstream of mechano-sensing processes such as those involving integrins, or if FAK is also per se exposed to and activated by mechanical force.

We here hypothesize that mechanical force acts as a direct stimulus of FAK activity, indications for which are two-fold. First, FAK is tethered between the PIP_2-enriched membrane and the cytoskeleton, likely acting as a force-carrying link in FAs. Second, the FERM-kinase structure suggests itself as a mechano-responsive scaffold, in which force could specifically detach the autoinhibitory FERM domain from the active site. FAK would be the first mechanoenzyme of FAs, allowing a direct transduction of a mechanical signal into an enzymatic reaction and downstream events into the nucleus, which would yield a mechanistic explanation of FAK's mechano-sensing role [10]. Indeed, two analogous cases of mechanically activated enzymes have been previously identified, both of which are kinases and feature force-induced activation by removal of an autoinhibitory domain, namely titin and twitchin kinase in muscle [34–36]. In contrast to the FAT domain [37], the force response of the autoinhibited FERM-kinase fragment is currently unknown. To test the hypothesis of FAK as a force-sensor, we performed extensive equilibrium molecular dynamics (MD) and force-probe molecular dynamics (FPMD) simulations of the FERM-kinase fragment of FAK under various conditions. Force propagating onto FAK from a PIP_2-enriched membrane and the cytoskeleton specifically opens the hydrophobic FERM-kinase interface, preparing FAK for activation via phosphorylation prior to the unfolding of the kinase domain. Given the low stability of the largely α-helical kinase and FERM domains, this is remarkable. The enforced activation is robust with regard to

a large range of pulling velocities, but sensitive to the site of force application. Our force-induced activation pathway suggests a direct mechanoenzymatic function of FAK in FAs.

Materials and Methods

Equilibrium MD simulations of the FERM-kinase fragment (FK-FAK) fragment [14] (PDB code: 2J0J) in the apo state, both in the absence and in the presence of a membrane containing PIP$_2$ and POPE lipids, as well as of only the membrane, were performed using the GROMACS package [38]. FPMD simulations [39, 40] of FK-FAK without a membrane were performed by subjecting the C-terminal C-alpha atom and the center-of-mass of the C-alpha atoms of the basic patch ^{216}KAKTLR^{221} to harmonic-spring potentials which were moved away from each other with constant velocity. FAT has been suggested to interact with FERM, binding to the same site as PIP2 does [41]. However, PIP2 binding is required for FAK activation [18, 19], thus excluding the possibility of FAT-FERM stable interactions for PIP2-mediated FAK activation. Other interactions between FAT and the FERM/Kinase complex are not known or at least suggested to be very dynamic and weak [42], and thereby easier to break under force conditions. This suggests that under tensile force, FAT is maintained sufficiently far from the complex, and that the force is transduced towards the complex through the fully-stretched 200 amino-acid proline-rich disordered linker. In consequence, in our FPMD simulations neither FAT nor the linker were considered.

The force response of membrane-bound FK-FAK was investigated by subjecting its C-terminus to a harmonic potential that was then moved away from the membrane either vertically or diagonally, while keeping the membrane position at its original position. PLS-FMA [43] was used to detect collective motions maximally correlated with the opening of the FERM-kinase interface. The underlying free energy landscape was characterized by analyzing the rupture forces as a function of loading rate, using both the HS model by Hummer & Szabo [44] and the BSK model by Bullerjahn et al. [45]. Kinetic models were based on previous biochemical networks [46–49] and simulated using COPASI [50]. Details of the methods are given in S1 Text.

Results

Force-induced release of FAK autoinhibition

In vitro, phosphorylation of the activation loop of FAK is enhanced by relieving the autoinhibition through Y180/M183 mutation [14] or PIP$_2$-binding [18]. Catalytic turnover of wild-type FAK, however, requires an additional biochemical stimulus. Here, we ask if mechanical force could promote full domain dissociation of FAK as required for auto- and Src-phosphorylation–analogous to the effect of the Y180/M183 mutation. We examined the effect of tensile force on the autoinhibited FK-FAK using FPMD simulations. Tethering FAK between the membrane and the cytoskeleton results in force transmission from the membrane onto the basic patch of the FERM domain and from the paxillin-interacting FAT domain through the proline-rich linker onto the kinase C-terminus (Fig 1A). Accordingly, in our simulations, a pulling force was applied to the basic patch of FERM and the C-terminus of the kinase domain in opposite directions with 13 different pulling velocities from 6×10^{-3} nm/ns to 1 nm/ns (1 in Fig 1B). For each pulling velocity, multiple runs were carried out (83 runs in total), yielding a concatenated simulated time of about 7 μs, with the slowest pulling simulation covering 1 μs. We observed the autoinhibitory FERM domain to dissociate from the kinase domain in 76 out of 83 FPMD simulations (more than 90% of the cases). Conformational damage of either the FERM F2-lobe or kinase C-lobe occurred in the remaining 7 simulations. Release of Tyr576/577 from FERM occurred always later, i.e. at larger end-to-end distances, than dissociation of the F2-lobe from the C-lobe (Fig 1B and 1C), suggesting the F2-C detachment to be a requirement for mechanical

FAK activation. We observed partial unfolding at the kinase C-terminus prior to exposure of Tyr576/577 to an only minor extent and mostly at higher loading rates, comprising at most a 15 nm increase in end-to-end length (Fig 1*B* and 1*C*), or no more than 30 residues of the C-terminal α-helix (S1 Fig). As the second half of this helix (or more) is typically disordered in other kinases (e.g. in protein kinase A or Src), its partial unfolding under force is likely not to impair FAK enzymatic function. Hence, our data suggest domain-domain dissociation to largely thwart the unfolding of the moderately stable α-helical domain structures. However, more substantial unfolding from the C-terminus of the kinase domain was the dominant pathway when pulling FK-FAK from its N and C-terminus (S2 Fig). Thus, we conclude that force acting specifically between the FERM basic patch and the kinase C-terminus removes the inhibitory FERM domain and thereby facilitates kinase activation, instead of domain unfolding and kinase inactivation.

FAK-membrane interactions under force

At FAs, the specific interaction of the FERM basic patch with PIP2 is required for the anchoring of FK-FAK to the membrane. Other phospholipids only display background levels of binding [18]. In our previous study, we observed an allosteric change at the FERM-kinase interface upon PIP$_2$ binding to FK-FAK, but no full opening [18]. This raised the question if full domain opening under force, as observed for isolated FK-FAK in solution, also occurs when FK-FAK is anchored to a membrane via PIP$_2$. This would require both the PIP$_2$-containing membrane as well as the PIP$_2$-FERM link to be mechanically more robust against rupture than the FERM-kinase interaction. To test this, we set up a palmitoyloleoylphosphatidylethanolamine (POPE) membrane containing 15% (mol/mol) of PIP$_2$ in the inner leaflet of the membrane, which was surrounded by water and neutralized by CaCl$_2$. Within 100 ns of MD simulations starting from individual PIP$_2$ molecules in the membrane, we observed the formation of small PIP$_2$ clusters involving two or more lipids and Ca^{2+} (S3 Fig), accompanied by a decrease of area per lipid by ~ 1 Å^2 (S1 Table), in agreement with divalent-cation-mediated PIP$_2$-enrichment in membranes [18, 24, 51]. FK-FAK was anchored to the membrane and the dynamics of the resulting complex was monitored over 150 ns of MD. Anchorage further increased clustering. The protein remained stably bound to the membrane through the FERM-PIP$_2$ and additional interactions between the kinase C-lobe and the membrane, independent from the initial orientation of the protein relative to the membrane plane (Fig 2*A* *left* and S3 Fig). The same was observed for a membrane with 1% PIP$_2$, which, however, showed less clustering and provided only a single PIP$_2$ lipid for anchorage of FK-FAK.

Next, we monitored the mechanical response of membrane-anchored FK-FAK. In FPMD simulations, we subjected the protein to force by moving a harmonic spring attached to the kinase C-terminus with constant velocity along a direction vertical or diagonal to the membrane, while position restraining the center-of-mass of the membrane bilayer (Fig 2*A*). At 15% PIP$_2$ concentration, independent of the pulling direction, we observed a loss of contacts of the kinase domain with the membrane and with the FERM domain, while the FERM-membrane interaction remained intact (Fig 2*B*). While diagonal pulling led to a concurrent dissociation of the kinase from the membrane and the FERM domain, vertical pulling resulted in kinase-membrane dissociation prior to kinase-FERM dissociation. In none of these simulations, we observed kinase unfolding prior to dissociation. Also, for both pulling directions, the membrane and the PIP$_2$-FERM interaction were mechanically more robust than those at the FERM-kinase interface. Thus, the membrane simulations reproduced the process predominantly observed for isolated FK-FAK in solution (compare Fig 2*B* with Fig 1*B* and 1*C*). Namely, they all showed force-induced removal of the autoinhibitory FERM domain and exposure of the activation loop carrying the Tyr576/577 phosphorylation site.
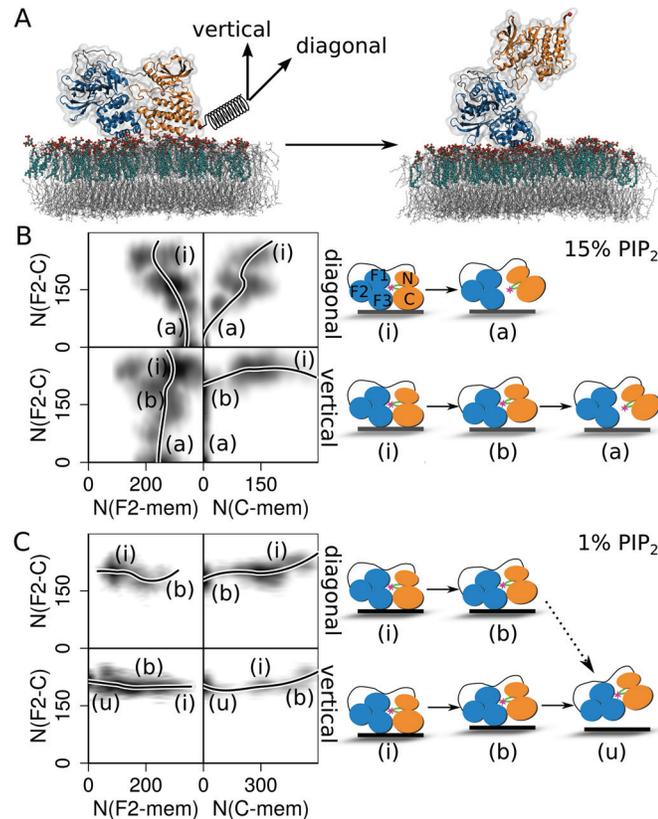
Fig 2. Mechanical activation of FAK bound to the membrane. A) Force was applied to the C-terminus of FK-FAK, in vertical or diagonal direction with respect to the membrane, with a counter-force acting on the membrane, leading to the release of autoinhibition (left to right transition). FK-FAK is shown as in Fig 1B, PIP$_2$ lipids in the membrane (here at 15%) in cyan/red and POPE lipids in grey. B-C) Number of contacts N between the FERM F2-lobe (F2) and the kinase C-lobe (C) compared to the number of contacts between both lobes and the membrane (mem), at 15% (B) and 1% (C) PIP$_2$ concentration. Number of contacts between lobes was defined as the number of atoms in one of the lobes closer than 0.6 nm to at least one atom of the other lobe. Upper panels show results for diagonal pulling while lower panels for vertical pulling. Densities of N (for a pulling velocity of 0.03 nm/ns) are shown as a grey gradient, with a polynomial fit to the data shown as a solid black line. The labels i, a, b, and u correspond to the inactive, active, bound and unbound states of FK-FAK, respectively, sketched at the right side.

doi:10.1371/journal.pcbi.1004593.g002

When we applied force to FK-FAK anchored to a membrane containing only 1% PIP$_2$, i.e. to a single PIP$_2$ molecule, detachment of the kinase domain from the membrane was followed by the detachment of also the FERM domain (Fig 2C). Full loss of membrane anchoring naturally stops force transmission and impedes activation. Thus, an interaction of the FERM basic patch with multiple PIP$_2$, which is likely in PIP$_2$-enriched membranes, is required for mechanical FK-FAK activation. This is in line with the fact that PIP5K overexpression increases and PIP5K knockdown decreases the open FAK conformation [19]. The pulling direction, instead, appears to be less relevant.

Mechanism of force-induced FK-FAK opening

We next analyzed in further detail the dynamics underlying the force-triggered FK-FAK domain-domain rupture. Applying partial least squares functional mode analysis (PLS-FMA) [43] to the simulations of isolated FK-FAK in solution, we obtained a collective opening

motion that maximally correlates with the increase in minimal distance between the F2 and C lobes (S4 Fig). This opening motion also strongly correlated with the F2-C lobe distances obtained for the trajectories of membrane-bound FK-FAK, suggesting that it captures the essential opening dynamics of FK-FAK both isolated and bound to the membrane. This implies the simplified system of isolated FK-FAK in solution to follow a FERM-kinase dissociation mechanism, which is highly similar to the one of the more realistic system including the membrane, even though it lacks effects from FERM/kinase-membrane interactions.

We then identified the first steps along the opening motion of FK-FAK giving rise to rupture forces. Fig 3A shows typical force profiles and F2/C-lobe interaction areas as a function of the spring locations recovered from the FPMD simulations. For both FK-FAK in isolation and bound to the membrane, and independent of the loading rate, we observed that the interface area between the two lobes was reduced in two steps, both of which coincided with noticeable force peaks. The maximal force was reached when the first decrease in inter-lobe area occurred
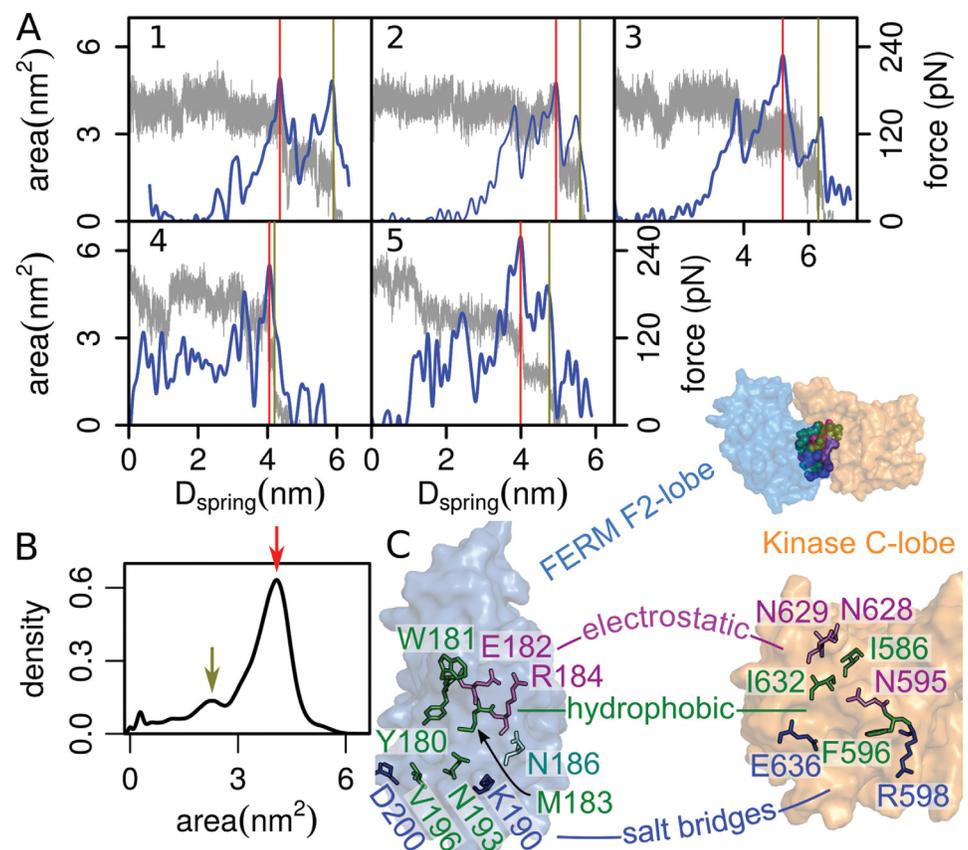
Fig 3. Mechanism of FK-FAK mechanical activation. A) Interfacial area between the F2- and C-lobe (grey) and average force exerted by the two springs (blue) as a function of the distance between springs, D_{spring}. Results from six independent FPMD simulations are shown: (1–3) without the membrane pulling at V = 0.006, 0.006 and 0.014 nm/ns, respectively, and (4 and 5) pulling diagonally away from the membrane at V = 0.03 and 0.05 nm/ns, respectively. The interfacial area drops from initial values of 3–4.5 nm^2 to intermediate values of 1.5–2.8 nm^2. Afterwards it decreases to zero. Rupture force (highest force peak) always corresponded to the first drop in the interfacial area (red line). The peak force associated to the second drop in the area is highlighted with the green line. B) Distribution of interface areas reflecting the two states of FK-FAK during its force-induced opening (highlighted with arrows). All FPMD simulations were considered to compute the distribution. C) Residues involved in the rupture steps are highlighted as sticks. FERM F2- and Kinase C-lobe are shown in surface representation. Rupture steps are associated to the disruption of hydrophobic interactions (green); salt bridges (blue) and other electrostatic interactions (magenta), and interactions with other partners (cyan). Residues were identified by TRFDA (S5 Fig). They are listed in S2 Table.

doi:10.1371/journal.pcbi.1004593.g003

(from 3–4.5 nm^2 to 1.5–2.8 nm^2). This led to a short-lived intermediate, as reflected by a second peak in the distribution of the F2/C-lobe interface area (Fig 3B), before the two lobes fully dissociated. We note that the intermediate becomes less evident for faster pulling velocities.

To pinpoint the load-carrying residue-residue interactions across the interface, we calculated the punctual stress of each residue, using time resolved force distribution analysis (TRFDA) [52], and thereby detected the loss of inter-lobe interactions during pulling (see S5 Fig, S2 Table, and S1 Text). Inter-lobe interactions which ruptured reproducibly at one of the two dissociation steps are highlighted in Fig 3C. The first major rupture step required the breakup of a hydrophobic cluster composed of residues Y180, M183, N193, V196, and F596, and of an additional salt bridge (D200-R598). Rupture of these interactions gave rise to the maximal force, thus stressing their critical stabilizing role. Our results are in agreement with the observation that mutations Y180A, M183A, and F596D result in constitutively active FAK with an open FERM-kinase interface [14, 18]. Residue pairs rupturing at the second step included residues of mostly electrostatic nature (E182, R184, K190 and N595, N628, N629, E636) and are located further away from the membrane anchor. This second rupture step is immediately followed by the opening of the remaining FERM-kinase interface established between the F1 and the N-lobe, including the exposure of Tyr576/577. Thus, the rupture process resembles a zipper-like mechanism, during which the FERM and kinase interface is sequentially opened. Herein, the membrane-proximal hydrophobic patch around F596 represents the most robust mechanical clamp to be opened first. Our PLS-FMA calculations further support this sequential mode of opening (S4C Fig).

Force required for FAK activation

Are the forces predicted by the simulations to relieve FAK autoinhibition relevant to FAK at FAs? At thirteen different loading rates, covering two orders of magnitude, we obtained maximal rupture forces for FK-FAK activation between 150 and 450 pN (Fig 4A). This force regime is similar to the one observed for titin kinase (400 pN at 0.2 pN/ps), a kinase known to be mechanically activated by forces present in muscle [35, 36, 53]. Our rupture forces are also similar to or slightly higher than those predicted by MD simulations of the focal adhesion proteins talin and vinculin (250–400 pN for nanosecond scale activation of talin [54, 55] and 100 pN for sub-nanosecond activation of vinculin [56], respectively). We then used both the HS model [44] and the BSK model [45] to fit the observed rupture forces as a function of the loading rate. This provided us with a set of compatible model parameters ΔG, D and x_b, where ΔG denotes the activation energy, D the effective diffusivity and x_b the separation between the inactive state and the transition state. Focusing on those parameter combinations that correspond to a physiologically plausible spontaneous activation rate of no more than $k_0 = 10^{-3}$ Hz, we obtained a number of best-fit estimates from which we derived the force-dependent activation rate $k(F)$ used in our kinetic model (Fig 4A and S6 Fig). We note that model parameters corresponding to an unphysiologically high spontaneous dissociation rate can improve our fit to the observed force fluctuations (S7 and S8 Figs). On this basis it might be speculated that there exists a second energy barrier at a larger value of x_b that guarantees thermal stability at low forces, but vanishes under the high forces used in our MD simulations. Nevertheless, this does not invalidate our qualitative findings on FK-FAK activation as force sensitivity increases exponentially with the barrier location x_b (see the S1 Text for a more detailed analysis).

Discussion

We here provide computational evidence for a force-induced activation mechanism of FAK, in which tensile force relieves the blockage of its active site, as well as its central Tyr576/577
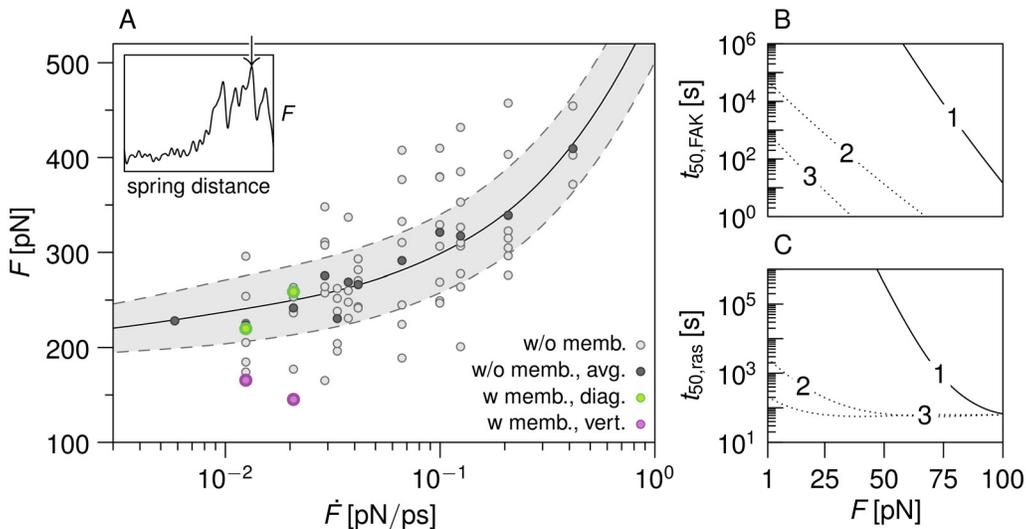
Fig 4. FAK mechano-signaling. A) Rupture force F as a function of the loading rate $\dot{F}$, where F is defined as the maximal force observed during FK-FAK activation (arrow in the inset). Light grey dots represent individual rupture forces F observed in our membrane-free FPMD simulations. Dark grey dots represent their averages (for each loading rate $\dot{F}$). The solid line shows the mean rupture force $\langle F \rangle$ predicted by the BSK model [45] for $\Delta G = 28.5\ k_B\ T$, $x_b = 0.86$ nm, and $D = 6.6 \times 10^6$ nm^2/s. A fit with the HS [44] model yields similar model parameters (not shown). Dashed lines show the variation of the rupture forces predicted by the BSK model (2 standard deviations, see S1 Text for a detailed analysis). Pulling membrane-bound FK-FAK diagonally yielded similarly large rupture forces (green dots). Vertical pulling resulted in significantly lower rupture forces (pink dots), as this direction promotes the less resistant zipper-like dissociation mechanism described in S4B and S4C Fig) Time at which 50% of inactive FAK (B) and GDP-bound Ras protein (C) are consumed, under varying external force. Times obtained for three sets of parameters (1 to 3) corresponding to the three fits presented in S6 Fig.

doi:10.1371/journal.pcbi.1004593.g004

phosphorylation site, imposed by the autoinhibitory FERM domain. The release of autoinhibition is likely to make the kinase active site accessible for its substrate, Tyr397 of the same or another FAK molecule [42, 57], and/or to render Tyr576/577 accessible to Src. It is non-trivial that the exertion of a pulling force at opposite sites of the FERM and kinase domains leads to their dissociation. Other likely scenarios are protein unfolding and PIP$_2$-protein dissociation, both of which would inactivate FAK, because an intact kinase structure and also PIP$_2$ binding [18] are required for FAK activity. In fact, α-helical proteins are known to unfold at forces typically lower than β-sheet proteins [58], and both the kinase C-lobe and the FERM F2 domain feature mainly α-helical secondary structure. In this regard, force-induced FAK unfolding would be an expected result and was indeed preferred over FERM-kinase dissociation when pulling the FERM F1- or F3-lobe away from the kinase C-terminus. Instead, in the particular – and physiologically relevant– case that force is applied to the PIP$_2$ binding site and the kinase C-terminus, we found domain-domain dissociation to be strongly preferred over unfolding or membrane detachment, over a large range of pulling velocities, and robust with regard to the pulling direction and presence of membrane interactions. Thus, the α-helical regions subjected to the pulling force mostly refrain from unfolding, and they instead transduce the load to the F2/C-lobe interface, which readily opens prior to substantial kinase unfolding. We suggest that it is the zipper-like topology, with the force application sites both located at the membrane-proximal basis of the two domains, that mechanically weakens the domain interface, resulting in efficient FAK opening and activation. Force transduction through the two termini, in contrast, results in shearing the two domains relative to each other, making them less prone to dissociate. The lower mechanical resistance of zipper versus shear-type topologies has been described earlier (e.g. [53]), and FAK force-induced domain-domain rupture and activation appears to be another variation of this theme.

Our findings not only decidedly argue for a mechano-sensing function of FAK, but also emphasize the crucial role of the membrane in mechanotransduction. First, membrane binding allows force to propagate to the F2-lobe of FAK. Second, the FAK-membrane interaction withstood the external load only in the case of PIP$_2$-enriched membranes (15% PIP$_2$). In contrast, FAK detached from low PIP$_2$-content membranes. This supports the notion of PIP$_2$ clustering as a requirement for FAK activation at FAs [18, 51]. We note that FAK can be activated *in vitro* by the sole action of PIP$_2$ and Src, i.e. in the absence of tensile forces acting on membrane-bound FAK at FAs in stretched cells. However, it has become clear that FAK activation can proceed along different routes, depending on the cellular environment, and potentially can also involve pH changes [59], and/or growth factor receptors [16]. We here propose force to substitute or complement some of these activators shaping the multi-dimensional landscape of FAK activity.

Using TRFDA, we recovered the stabilizing role of Y180, M183, V196 and F596, a hydrophobic core previously shown by mutagenesis to stabilize the autoinhibited state [14], validating our simulation data. In addition, we found D200 and R598 to contribute to the rupture force, and predict their mutation to result in increased FAK activity.

The question arises, how force feeds into FAK-mediated Ras GDP/GTP exchange and regulates ERK-dependent gene expression, analogous to the chemical stimulation of growth factor receptor-dependent Ras signaling (S9 Fig) [27]. To assess how FAK as a mechanosensor couples mechanical signals into the downstream biochemical network, we defined force-dependent FAK activation as the initial step of a kinetic model for the Ras signaling pathway (S10 Fig) [46–49]. Both FAK opening and GDP/GTP exchange in Ras are accelerated by external forces, as expected (Fig 4B and 4C and S11A Fig). Intriguingly, while FAK force-induced activation shows a nearly linear dependency on force on the logarithmic scale (Fig 4B), Ras-GTP production shows a highly non-linear dependency and saturates beyond a critical force (Fig 4C). The reason is that activated FAK in complex with its partners, Grb2 and SOS via c-Src and SHC, acts as an enzyme for Ras activation. As a direct consequence, Ras activation follows mechano-enzymatic kinetics reminiscent of an inhibitory Michaelis-Menten mechanisms (S11B Fig) [60], in which force regulates the enzyme concentration.

In conclusion, our computational study provides direct evidence at the molecular level for a mechano-sensory role played by FAK at PIP$_2$-enriched membranes of FAs. Through a specific domain opening mechanism regulated by force, FAK can integrate mechanical and chemical stimuli into downstream signaling to the nucleus. We suggest the mechano-enzymatics of FAK and Ras to provide a cap on the cell's mechano-response. Our results, on FAK activation and signaling, are directly testable among others by molecular force sensors [61, 62] and cell stretching experiments. How other putatively mechano-activated kinases, such as the related Src kinase, follow similar mechanisms, at focal adhesions or elsewhere, remains to be shown.

Supporting Information

S1 Fig. Partial unfolding of the kinase domain. A) Distance between the pulled groups at the moment of dissociation (D$_{e-e}$) as a function of the applied loading rate. Dissociation was monitored between the FERM F2-lobe and the kinase C-lobe (F2-C) and between the FERM domain and the Tyr576–577 phosphorylation site (F-YY). Each dot corresponds to one simulation run and the line is a polynomial fit to all the points as a guide to the eye, indicating a slight augment in D$_{e-e}$ with increasing loading rate. B) Number of unstructured residues N$_{UN}$ as a function of the time, for a simulation displaying a large D$_{e-e}$ value (circle in A). Time trace is shown in black and a polynomial fit as a guide to the eye in blue. Residual unfolding of around 30 residues was observed at the C-terminus. The number of unstructured residues was obtained using

VMD [63]. The inset shows the conformation of the Kinase domain at the moment of dissociation (at 42 ns, green line). Despite of the high loading rate, the conformation of the Kinase domain remained almost intact (unfolded residues of its C-terminus are highlighted in red). (EPS)

S2 Fig. Unfolding is preferred over dissociation of FK-FAK when exerting force to the FERM F1 or F3 lobes. The number of unfolded amino acids at the C-terminus of the FAK kinase domain is shown as a function of the number of contacts between the FERM F2- and the kinase C-lobe. Density recovered from the simulations is shown with the gray scale and polynomial fit with the black line. External force was applied to the N-terminus of the FERM F1-lobe (left) or the COM of the FERM F3-lobe (right). This is in contrast to the pathway observed in the majority of the simulations applying force to the basic patch of the FERM F2-lobe, in which only minor unfolding was observed before dissociation (up to 30 residues, see S1 Fig). (EPS)

S3 Fig. PIP$_2$ interactions are mediated by calcium ions. Snapshots of a lipid bilayer in the absence (upper panels) and in the presence (lower panels) of FK-FAK. Snapshots were extracted from equilibrium MD simulations at the indicated times. 15% PIP$_2$ lipids (yellow) are embedded in a palmitoyloleoylphosphatidylethanolamine (POPE) lipid bilayer (light red and periodic images in black). PIP$_2$ formed clusters (dark red) mediated by Ca^{2+} ions (green). This caused a decrease in the area per lipid (see S1 Table). Clustering was less pronounced for lower PIP$_2$ concentrations (see S1 Table). Lower right panel illustrates the FK-FAK bound to the bilayer, with the basic patch (cyan) at the FERM domain (blue) tethered to one of the PIP2-Ca^{2+} clusters (only this cluster is shown for clarity). The kinase domain (orange) also established interactions with the bilayer (red surface). (EPS)

S4 Fig. Partial least square functional mode analysis (PLS-FMA) to compare the force-induced dissociation mechanism of FK-FAK at different loading rates, in presence and absence of the membrane. A) Minimum distance between the F2- and C-lobe observed in FPMD simulations (black) compared to that predicted by PLS-FMA (color). To build the model (i.e. obtain the collective motion that is maximally correlated with the F2-C distance) the first half of the non-membrane FPMD simulations was considered (red). To validate the resulting model, the remaining part of these trajectories (green, model validation I), as well as, trajectories of FPMD simulations including membrane (blue, model validation II), were considered. B) Correlation coefficient between the minimum distance between the F2- and C-lobe predicted by PLS-FMA as a function of the number of PLS components. Same color coding as A. High correlation (> 0.9) was obtained both for the model and the the two validation data sets. Predictions in A correspond to the situation using 11 PLS components. C) Predicted ensemble-weighted motion of FK-FAK from its closed form (cyan) to its open form (gray), resembling a zipper-like motion. (EPS)

S5 Fig. Residue stresses during dissociation reveal critical residues for inter-domain stability of FK-FAK. Punctual stresses due to inter-lobe interactions of residues in the FERM domain (residues 175–245) and the kinase domain (residues 586–666) are shown as a function of spring distance during individual FPMD simulations. Punctual stresses were calculated using time resolved force distribution analysis (TRFDA, see S1 Text). Color coding according to the gray scale bar at the side. The red line indicates the distance between springs at which the highest force peak was observed. This event correspond to the transition of FK-FAK from

the inactive to an intermediate state. The green line highlights the moment at which a second rupture event is observed, rendering FK-FAK activation. Punctual stresses are depicted for three FPMD simulations of FK-FAK isolated and in solution (A-C), at low pulling velocities, and for two FPMD simulations of FK-FAK bound to the membrane (D-E), pulling in diagonal direction from the membrane. Stresses are only shown for residues with significantly large stress values, and these residues varied among simulations. Residues that consistently showed pronounced drops in punctual stress upon rupture are listed in S2 Table and displayed in Fig 3C. of the main text.
(EPS)

S6 Fig. Parameter space topography. A) least-squares fits of $\langle F \rangle$ to the data allow for a wide range of model parameters ΔG and x_b. Fit computed via the BSK model. The HS model yields virtually identical results. Within the dark blue region, the RMSD error $\delta \langle F \rangle$ remains below 15 pN. As the effective transducer stiffness κ_s might be further reduced by the finite stiffness of the C-terminus and the FERM domain, we have successively reduced κ_s until we were no longer able to produce a good fit (lowest effective stiffness $0.01 \kappa_s$ shown in orange). Black dotted lines show the force-induced increase in the unbinding rate at F = 50 pN, as evaluated using Eq. 6 of S1 Text. For the kinetic model, we only consider parameter combinations $(D, \Delta G, x_b)$ that yield a reasonably low spontaneous dissociation rate $k_0 < 10^{-3}$ s^{-1} (evaluated for $D = 10^6$ nm^2/s. $k_0 = 10^{-3}$ s^{-1} boundary indicated by the red dashed line. B) representative rupture force fits, evaluated using the model parameters (and corresponding stiffnesses κ_s indicated in (A) and Fig 4 in the main text.
(EPS)

S7 Fig. Unconstrained rupture force fitting. Dropping the requirement of thermal stability, we obtain a best-fit parameter set $D = 1.2 \times 10^7$ nm^2/s, $\Delta G = 14.2 k_B T$, $x_b = 0.3$ nm that corresponds to unphysiologically large spontaneous activation rates $k_0 > 1$ s^{-1}, but produces a better fit to the observed rupture force spectra.
(EPS)

S8 Fig. Bayesian parameter estimation. A) Lower panel: assuming a logarithmic prior distribution $p_i = p_{i,1} \propto [\Delta G \times x_b \times D]^{-1}$ and integrating out D, we obtain a joint probability distribution for ΔG and x_b that is shown here for transducer stiffnesses of $\kappa_s = 250$ kJmol^{-1}nm^{-2} (blue) and $0.1 \kappa_s = 25$ kJmol^{-1}nm^{-2} (orange), respectively. Dark shaded areas enclose 50% of the corresponding parameter probability distributions, light shaded regions enclose 95%. Upper panel: marginal probability distributions for ΔG obtained by integrating out both D and x_b. B) same as A, but evaluated for a uniform prior distribution $p_i(\Delta G, x_b, D) = p_{i,2}(\Delta G, x_b, D) = $ const.
(EPS)

S9 Fig. Kinetic scheme of FAK signaling regulated by external force. Numbering of individual reactions is arbitrary.
(EPS)

S10 Fig. A scheme of the ERK/MAPK signaling pathway. Chemical signals such as EGF binding to RTK in the cell membrane induce autophosphorylation in the cytoplasmic domain of RTK. Then, through sequential phosphorylation of a number of downstream proteins, the signal is transduced into the cell nucleus. Mechanical signals act on the cell membrane and trigger the activation of the non-receptor tyrosine kinase, FAK, which is located at the cytoplasmic face of the membrane bilayer. Activated FAK thus mediates the signal transduction into the cell nucleus through a pathway constituted by a chain of similar interactions.
(EPS)

S11 Fig. Downstream FAK signaling. A) Time course of FAK opening and the GDP/GTP exchange in the Ras protein obtained with varying external forces in a range between 1 and 100 pN (along the direction pointed by the blue arrow). Decrease in the concentration of closed FAK (black) and decrease in the concentration of GDP bound Ras protein (red) are shown. Time at which 50% of both GDP-bound Ras protein and closed FAK are consumed is highlighted with the dashed line. These values are shown as a function of applied force in Fig 4B and 4C of the main text. B) Rate of the GDP/GTP reaction as a function of the Ras-GDP concentration obtained for increasing external forces indicated with the blue arrow.
(EPS)

S1 Table. Membrane structural properties at different PIP$_2$ lipid concentrations.
(EPS)

S2 Table. Probability for residues in the FERM (left) and the kinase (right) domain to lose their interaction (in one of the two major dissociation steps, step 1 or 2, or elsewhere), based on TRFDA (S5 Fig). Residues dominating the first rupture step are labeled with * (hydrophobic interactions), ‡ (salt bridges) and § (varying partners), and residues dominantly involved in the second step in † (mostly electrostatic interactions). These residues are displayed in Fig 3C of main text.
(EPS)

S1 Text. Supporting text.
(PDF)

Acknowledgments

Author Contributions

Conceived and designed the experiments: CAS AB FG. Performed the experiments: JZ. Analyzed the data: JZ CAS SS JTB FG. Contributed reagents/materials/analysis tools: JZ CAS SS JTB. Wrote the paper: JZ CAS SS FG.

References

1. Vogel V, Sheetz M. Local force and geometry sensing regulate cell functions. Nat Rev Mol Cell Biol. 2006 Apr; 7(4):265–275. doi: 10.1038/nrm1890 PMID: 16607289

2. Schiller HB, Fässler R. Mechanosensitivity and compositional dynamics of cell-matrix adhesions. EMBO Rep. 2013 Jun; 14(6):509–519. doi: 10.1038/embor.2013.49 PMID: 23681438

3. Oakes PW, Gardel ML. Stressing the limits of focal adhesion mechanosensitivity. Curr Opin Cell Biol. 2014 Oct; 30:68–73. doi: 10.1016/j.ceb.2014.06.003 PMID: 24998185

4. Kanchanawong P, Shtengel G, Pasapera AM, Ramko EB, Davidson MW, Hess HF, et al. Nanoscale architecture of integrin-based cell adhesions. Nature. 2010 Nov; 468(7323):580–584. doi: 10.1038/nature09621 PMID: 21107430

5. Zhu J, Luo BH, Xiao T, Zhang C, Nishida N, Springer TA. Structure of a complete integrin ectodomain in a physiologic resting state and activation and deactivation by applied forces. Mol Cell. 2008 Dec; 32 (6):849–861. doi: 10.1016/j.molcel.2008.11.018 PMID: 19111664

6. del Rio A, Perez-Jimenez R, Liu R, Roca-Cusachs P, Fernandez JM, Sheetz MP. Stretching single talin rod molecules activates vinculin binding. Science. 2009 Jan; 323(5914):638–641. doi: 10.1126/science.1162912 PMID: 19179532

7. Sawada Y, Tamada M, Dubin-Thaler BJ, Cherniavskaya O, Sakai R, Tanaka S, et al. Force sensing by mechanical extension of the Src family kinase substrate p130Cas. Cell. 2006 Dec; 127(5):1015–1026. doi: 10.1016/j.cell.2006.09.044 PMID: 17129785

8. Schaller MD. Cellular functions of FAK kinases: insight into molecular mechanisms and novel functions. J Cell Sci. 2010 Apr; 123(Pt 7):1007–1013. doi: 10.1242/jcs.045112 PMID: 20332118

9. Zhao J, Guan JL. Signal transduction by focal adhesion kinase in cancer. Cancer Metastasis Rev. 2009 Jun; 28(1–2):35–49. doi: 10.1007/s10555-008-9165-4 PMID: 19169797

10. Vadali K, Cai X, Schaller MD. Focal adhesion kinase: an essential kinase in the regulation of cardiovascular functions. IUBMB Life. 2007 Nov; 59(11):709–716. doi: 10.1080/15216540701694245 PMID: 17968709

11. Schlaepfer DD, Mitra SK, Ilic D. Control of motile and invasive cell phenotypes by focal adhesion kinase. Biochim Biophys Acta. 2004 Jul; 1692(2–3):77–102. doi: 10.1016/j.bbamcr.2004.04.008 PMID: 15246681

12. Calalb MB, Polte TR, Hanks SK. Tyrosine phosphorylation of focal adhesion kinase at sites in the catalytic domain regulates kinase activity: a role for Src family kinases. Mol Cell Biol. 1995 Feb; 15(2):954–963. doi: 10.1128/MCB.15.2.954 PMID: 7529876

13. Cooper LA, Shen TL, Guan JL. Regulation of focal adhesion kinase by its amino-terminal domain through an autoinhibitory interaction. Mol Cell Biol. 2003 Nov; 23(22):8030–8041. doi: 10.1128/MCB.23.22.8030-8041.2003 PMID: 14585964

14. Lietha D, Cai X, Ceccarelli DFJ, Li Y, Schaller MD, Eck MJ. Structural basis for the autoinhibition of focal adhesion kinase. Cell. 2007 Jun; 129(6):1177–1187. doi: 10.1016/j.cell.2007.05.041 PMID: 17574028

15. Schaller MD. Paxillin: a focal adhesion-associated adaptor protein. Oncogene. 2001 Oct; 20(44):6459–6472. doi: 10.1038/sj.onc.1204786 PMID: 11607845

16. Chen SY, Chen HC. Direct interaction of focal adhesion kinase (FAK) with Met is required for FAK to promote hepatocyte growth factor-induced cell invasion. Mol Cell Biol. 2006 Jul; 26(13):5155–5167. doi: 10.1128/MCB.02186-05 PMID: 16782899

17. Plaza-Menacho I, Morandi A, Mologni L, Boender P, Gambacorti-Passerini C, Magee AI, et al. Focal adhesion kinase (FAK) binds RET kinase via its FERM domain, priming a direct and reciprocal RET-FAK transactivation mechanism. J Biol Chem. 2011 May; 286(19):17292–17302. doi: 10.1074/jbc.M110.168500 PMID: 21454698

18. Goñi GM, Epifano C, Boskovic J, Camacho-Artacho M, Zhou J, Bronowska A, et al. Phosphatidylinositol 4,5-bisphosphate triggers activation of focal adhesion kinase by inducing clustering and conformational changes. Proc Natl Acad Sci U S A. 2014 Aug; 111(31):E3177–E3186. doi: 10.1073/pnas.1317022111 PMID: 25049397

19. Cai X, Lietha D, Ceccarelli DF, Karginov AV, Rajfur Z, Jacobson K, et al. Spatial and temporal regulation of focal adhesion kinase activity in living cells. Mol Cell Biol. 2008 Jan; 28(1):201–214. doi: 10.1128/MCB.01324-07 PMID: 17967873

20. Di Paolo G, Pellegrini L, Letinic K, Cestra G, Zoncu R, Voronov S, et al. Recruitment and regulation of phosphatidylinositol phosphate kinase type 1 gamma by the FERM domain of talin. Nature. 2002 Nov; 420(6911):85–89. doi: 10.1038/nature01147 PMID: 12422219

21. Ling K, Doughman RL, Firestone AJ, Bunce MW, Anderson RA. Type I gamma phosphatidylinositol phosphate kinase targets and regulates focal adhesions. Nature. 2002 Nov; 420(6911):89–93. doi: 10.1038/nature01082 PMID: 12422220

22. McLaughlin S, Murray D. Plasma membrane phosphoinositide organization by protein electrostatics. Nature. 2005 Dec; 438(7068):605–611. doi: 10.1038/nature04398 PMID: 16319880

23. van den Bogaart G, Meyenberg K, Risselada HJ, Amin H, Willig KI, Hubrich BE, et al. Membrane protein sequestering by ionic protein-lipid interactions. Nature. 2011 Nov; 479(7374):552–555. doi: 10.1038/nature10545 PMID: 22020284

24. Ellenbroek WG, Wang YH, Christian DA, Discher DE, Janmey PA, Liu AJ. Divalent cation-dependent formation of electrostatic PIP2 clusters in lipid monolayers. Biophys J. 2011 Nov; 101(9):2178–2184. doi: 10.1016/j.bpj.2011.09.039 PMID: 22067156

25. Carvalho K, Ramos L, Roy C, Picart C. Giant unilamellar vesicles containing phosphatidylinositol(4,5) bisphosphate: characterization and functionality. Biophys J. 2008 Nov; 95(9):4348–4360. doi: 10.1529/biophysj.107.126912 PMID: 18502807

26. Giannone G, Rondé P, Gaire M, Beaudouin J, Haiech J, Ellenberg J, et al. Calcium rises locally trigger focal adhesion disassembly and enhance residency of focal adhesion kinase at focal adhesions. J Biol Chem. 2004 Jul; 279(27):28715–28723. doi: 10.1074/jbc.M404054200 PMID: 15102844

27. Tomakidi P, Schulz S, Proksch S, Weber W, Steinberg T. Focal adhesion kinase (FAK) perspectives in mechanobiology: implications for cell behaviour. Cell Tissue Res. 2014 Sep; 357(3):515–526. doi: 10.1007/s00441-014-1945-2 PMID: 24988914

28. Li S, Kim M, Hu YL, Jalali S, Schlaepfer DD, Hunter T, et al. Fluid shear stress activation of focal adhesion kinase. Linking to mitogen-activated protein kinases. J Biol Chem. 1997 Nov; 272(48):30455–30462. doi: 10.1074/jbc.272.48.30455 PMID: 9374537

29. Li S, Butler P, Wang Y, Hu Y, Han DC, Usami S, et al. The role of the dynamics of focal adhesion kinase in the mechanotaxis of endothelial cells. Proc Natl Acad Sci U S A. 2002 Mar; 99(6):3546–3551. doi: 10.1073/pnas.052018099 PMID: 11891289

30. Wang HB, Dembo M, Hanks SK, Wang Y. Focal adhesion kinase is involved in mechanosensing during fibroblast migration. Proc Natl Acad Sci U S A. 2001 Sep; 98(20):11295–11300. doi: 10.1073/pnas.201201198 PMID: 11572981

31. Polacheck WJ, German AE, Mammoto A, Ingber DE, Kamm RD. Mechanotransduction of fluid stresses governs 3D cell migration. Proc Natl Acad Sci U S A. 2014 Feb; 111(7):2447–2452. doi: 10.1073/pnas.1316848111 PMID: 24550267

32. Chaturvedi LS, Marsh HM, Basson MD. Src and focal adhesion kinase mediate mechanical strain-induced proliferation and ERK1/2 phosphorylation in human H441 pulmonary epithelial cells. Am J Physiol Cell Physiol. 2007 May; 292(5):C1701–C1713. doi: 10.1152/ajpcell.00529.2006 PMID: 17215324

33. Seong J, Tajik A, Sun J, Guan JL, Humphries MJ, Craig SE, et al. Distinct biophysical mechanisms of focal adhesion kinase mechanoactivation by different extracellular matrix proteins. Proc Natl Acad Sci U S A. 2013 Nov; 110(48):19372–19377. doi: 10.1073/pnas.1307405110 PMID: 24222685

34. von Castelmur E, Strümpfer J, Franke B, Bogomolovas J, Barbieri S, Qadota H, et al. Identification of an N-terminal inhibitory extension as the primary mechanosensory regulator of twitchin kinase. Proc Natl Acad Sci U S A. 2012 Aug; 109(34):13608–13613. doi: 10.1073/pnas.1200697109 PMID: 22869697

35. Gräter F, Shen J, Jiang H, Gautel M, Grubmüller H. Mechanically induced titin kinase activation studied by force-probe molecular dynamics simulations. Biophys J. 2005 Feb; 88(2):790–804. doi: 10.1529/biophysj.104.052423 PMID: 15531631

36. Puchner EM, Alexandrovich A, Kho AL, Hensen U, Schäfer LV, Brandmeier B, et al. Mechanoenzymatics of titin kinase. Proc Natl Acad Sci U S A. 2008 Sep; 105(36):13385–13390. doi: 10.1073/pnas.0805034105 PMID: 18765796

37. Mofrad MRK, Golji J, Abdul Rahim NA, Kamm RD. Force-induced unfolding of the focal adhesion targeting domain and the influence of paxillin binding. Mech Chem Biosyst. 2004 Dec; 1(4):253–265. PMID: 16783922

38. Pronk S, Páll S, Schulz R, Larsson P, Bjelkmar P, Apostolov R, et al. GROMACS 4.5: a high-throughput and highly parallel open source molecular simulation toolkit. Bioinformatics. 2013 Apr; 29(7):845–854. doi: 10.1093/bioinformatics/btt055 PMID: 23407358

39. Grubmüller H, Heymann B, Tavan P. Ligand binding: molecular mechanics calculation of the streptavidin-biotin rupture force. Science. 1996 Feb; 271(5251):997–999. doi: 10.1126/science.271.5251.997

40. Sotomayor M, Schulten K. Single-molecule experiments in vitro and in silico. Science. 2007 May; 316 (5828):1144–1148. doi: 10.1126/science.1137591 PMID: 17525328

41. Kadaré G, Gervasi N, Brami-Cherrier K, Blockus H, Messari SE, Arold ST, et al. Conformational dynamics of the focal adhesion targeting domain control specific functions of focal adhesion kinase in cells. J Biol Chem. 2015 Jan; 290(1):478–491. doi: 10.1074/jbc.M114.593632

42. Brami-Cherrier K, Gervasi N, Arsenieva D, Walkiewicz K, Boutterin MC, Ortega A, et al. FAK dimerization controls its kinase-dependent functions at focal adhesions. EMBO J. 2014 Feb; 33(4):356–370. doi: 10.1002/embj.201386399 PMID: 24480479

43. Krivobokova T, Briones R, Hub JS, Munk A, de Groot BL. Partial least-squares functional mode analysis: application to the membrane proteins AQP1, Aqy1, and CLC-ec1. Biophys J. 2012 Aug; 103 (4):786–796. doi: 10.1016/j.bpj.2012.07.022 PMID: 22947940

44. Hummer G, Szabo A. Kinetics from nonequilibrium single-molecule pulling experiments. Biophys J. 2003 Jul; 85(1):5–15. doi: 10.1016/S0006-3495(03)74449-X PMID: 12829459

45. Bullerjahn JT, Sturm S, Kroy K. Theory of rapid force spectroscopy. Nat Commun. 2014; 5:4463. doi: 10.1038/ncomms5463 PMID: 25079911

46. Nguyen DH, Webb DJ, Catling AD, Song Q, Dhakephalkar A, Weber MJ, et al. Urokinase-type plasminogen activator stimulates the Ras/Extracellular signal-regulated kinase (ERK) signaling pathway and MCF-7 cell migration by a mechanism that requires focal adhesion kinase, Src, and Shc. Rapid dissociation of GRB2/Sps-Shc complex is associated with the transient phosphorylation of ERK in urokinase-treated cells. J Biol Chem. 2000 Jun; 275(25):19382–19388. Available from: http://dx.doi.org/10.1074/jbc.M909575199. PMID: 10777511

47. Schlaepfer DD, Jones KC, Hunter T. Multiple Grb2-mediated integrin-stimulated signaling pathways to ERK2/mitogen-activated protein kinase: summation of both c-Src- and focal adhesion kinase-initiated

tyrosine phosphorylation events. Mol Cell Biol. 1998 May; 18(5):2571–2585. doi: 10.1128/MCB.18.5.2571 PMID: 9566877

48. Kholodenko BN, Demin OV, Moehren G, Hoek JB. Quantification of short term signaling by the epidermal growth factor receptor. J Biol Chem. 1999 Oct; 274(42):30169–30181. doi: 10.1074/jbc.274.42.30169 PMID: 10514507

49. Hatakeyama M, Kimura S, Naka T, Kawasaki T, Yumoto N, Ichikawa M, et al. A computational model on the modulation of mitogen-activated protein kinase (MAPK) and Akt pathways in heregulin-induced ErbB signalling. Biochem J. 2003 Jul; 373(Pt 2):451–463. doi: 10.1042/BJ20021824 PMID: 12691603

50. Hoops S, Sahle S, Gauges R, Lee C, Pahle J, Simus N, et al. COPASI–a COmplex PAthway SImulator. Bioinformatics. 2006 Dec; 22(24):3067–3074. doi: 10.1093/bioinformatics/btl485 PMID: 17032683

51. James DJ, Khodthong C, Kowalchyk JA, Martin TFJ. Phosphatidylinositol 4,5-bisphosphate regulates SNARE-dependent membrane fusion. J Cell Biol. 2008 Jul; 182(2):355–366. doi: 10.1083/jcb.200801056 PMID: 18644890

52. Costescu BI, Gräter F. Time-resolved force distribution analysis. BMC Biophys. 2013; 6(1):5. doi: 10.1186/2046-1682-6-5 PMID: 24499624

53. Rief M, Gautel M, Oesterhelt F, Fernandez JM, Gaub HE. Reversible unfolding of individual titin immunoglobulin domains by AFM. Science. 1997 May; 276(5315):1109–1112. doi: 10.1126/science.276.5315.1109 PMID: 9148804

54. Lee SE, Kamm RD, Mofrad MRK. Force-induced activation of talin and its possible role in focal adhesion mechanotransduction. J Biomech. 2007; 40(9):2096–2106. doi: 10.1016/j.jbiomech.2007.04.006 PMID: 17544431

55. Hytönen VP, Vogel V. How force might activate talin's vinculin binding sites: SMD reveals a structural mechanism. PLoS Comput Biol. 2008 Feb; 4(2):e24. doi: 10.1371/journal.pcbi.0040024 PMID: 18282082

56. Golji J, Mofrad MRK. A molecular dynamics investigation of vinculin activation. Biophys J. 2010 Aug; 99(4):1073–1081. doi: 10.1016/j.bpj.2010.05.024 PMID: 20712990

57. Toutant M, Costa A, Studler JM, Kadaré G, Carnaud M, Girault JA. Alternative splicing controls the mechanisms of FAK autophosphorylation. Mol Cell Biol. 2002 Nov; 22(22):7731–7743. doi: 10.1128/MCB.22.22.7731-7743.2002 PMID: 12391143

58. Rief M, Pascual J, Saraste M, Gaub HE. Single molecule force spectroscopy of spectrin repeats: low unfolding forces in helix bundles. J Mol Biol. 1999 Feb; 286(2):553–561. doi: 10.1006/jmbi.1998.2466 PMID: 9973570

59. Ritt M, Guan JL, Sivaramakrishnan S. Visualizing and manipulating focal adhesion kinase regulation in live cells. J Biol Chem. 2013 Mar; 288(13):8875–8886. doi: 10.1074/jbc.M112.421164 PMID: 23393139

60. Bisswanger H. In: Enzyme Kinetics: Section 2.1–2.5. Wiley-VCH Verlag GmbH & Co. KGaA; 2008. p. 59–124. Available from: http://dx.doi.org/10.1002/9783527622023.ch2a.

61. Grashoff C, Hoffman BD, Brenner MD, Zhou R, Parsons M, Yang MT, et al. Measuring mechanical tension across vinculin reveals regulation of focal adhesion dynamics. Nature. 2010 Jul; 466(7303):263–266. doi: 10.1038/nature09198 PMID: 20613844

62. Wang X, Ha T. Defining single molecular forces required to activate integrin and notch signaling. Science. 2013 May; 340(6135):991–994. doi: 10.1126/science.1231041 PMID: 23704575

63. Humphrey W, Dalke A, Schulten K. VMD: visual molecular dynamics. J Mol Graph. 1996 Feb; 14(1):33–8, 27–8. doi: 10.1016/0263-7855(96)00018-5 PMID: 8744570